

## Research Note

# Simulating observable comets

## II. Simultaneous stellar and galactic action

P. A. Dybczyński

Astronomical Observatory of the A. Mickiewicz University, Słoneczna 36, 60-286 Poznań, Poland  
e-mail: dybol@amu.edu.pl

Received 28 April 2005 / Accepted 22 June 2005

**Abstract.** This is the second in a series of papers presenting an attempt to reproduce the mechanisms acting currently on the Oort cloud of comets (Oort 1950, Bull. Astron. Inst. Nether., 11, 91) and producing the observed sample of long-period comets. We combine the effect of the close, recent stellar passage with the continuous action of the Galactic tidal perturbation, and concentrate on the dominant term of this effect, namely the tidal force induced by the galactic disk matter. The main results presented in the previous paper of this series are fully confirmed within a much more realistic model. The results we obtained is that the observable subpopulation of the Oort cometary cloud remained the same in number, even after the close stellar passage. The main output of such a passage is a short time variation in the observable influx of comets and strong asymmetries present in their perihelion direction distribution.

**Key words.** comets: general – Oort cloud – solar system: general

### 1. Introduction

In the first paper of this series (Dybczyński 2002c, hereafter Paper I) we presented a detailed analysis of the separate stellar effect on the cometary cloud. We introduced two different numerical models of the cloud itself and calculated probabilities of various cometary end-states as a function of stellar passage geometrical and dynamical parameters. In addition, we discussed the asymmetries in the sample of the observable comets resulting from the stellar impulse on the cloud. The reader can find additional details of some peculiar cases in (Dybczyński 2002a,b). In the present paper we concentrate on the simultaneous action of the single stellar passage and of the Galactic disk tide. The main purpose of this paper is to demonstrate the results of a single stellar passage through or near the Oort cometary cloud under the simultaneous influence of galactic perturbations. In Sects. 2 and 3 we briefly present the nature and output of galactic perturbations, in Sect. 4 we discuss the way of superposition of stellar and Galactic perturbations, in Sect. 5 we describe “*dynamical filtering*”, an useful tool for speeding the calculations up, in Sect. 6 we present a detailed scheme of our Monte Carlo simulation code and finally in Sects. 7 and 8 we describe results of our simulations.

### 2. The nature of galactic perturbations

Among the first papers on the Galactic perturbations on Oort cloud comets one should mention those by Byl (1983, 1986),

Harrington (1985), Heisler & Tremaine (1986) and Matese & Whitman (1989). After recognizing that the tidal action of the galactic disk matter is about ten times stronger than the influence of the Galactic center, the simple dynamical model was proposed to omit the latter, giving the following set of equations of motion:

$$\begin{aligned}\ddot{x} &= -\frac{\mu x}{r^3}, \\ \ddot{y} &= -\frac{\mu y}{r^3}, \\ \ddot{z} &= -\frac{\mu z}{r^3} - 4\pi G\rho z.\end{aligned}\quad (1)$$

Here  $x, y, z$  are heliocentric comet coordinates in the galactic reference frame,  $G = k^2$ ,  $k = 0.01720209895$  being the Gaussian gravitational constant and  $\rho$  the local disk matter density. According to modern determinations (see for example: Holmberg & Flynn 2000), we adopt  $\rho = 0.1 M_{\odot} \text{pc}^{-3}$  in the present paper. In all calculations we describe the comet motion in the barycentric reference frame, so that

$$\mu = k^2 \cdot (1 + \sum m_p), \quad (2)$$

where  $m_p$  denotes planetary masses, expressed in the solar mass. This than gives  $\mu \simeq 1.00134 \cdot k^2$ .

In some recent papers on galactic perturbations on the Oort cloud comets (Levison et al. 2001; Brassier 2001; Matese & Lissauer 2002), the authors use the extended models for the Galactic perturbations, accounting for the perturbations

from the Galactic center. However, the simple model presented above is quite sufficient for our purpose. Inclusion of the influence of the Galactic center is not necessary here because we follow the cometary motion on relatively short time intervals of only several million years. Prętko (1998) has already shown that different models of the Galactic potential give significant differences only after a substantially longer time. For this reason the objections of Matese & Whitmire (1996) do not apply in our case.

The effects of the galactic disk tidal force on cometary motion described by Eqs. (1) were studied in detail in many papers; see for example Heisler & Tremaine (1986), Prętko & Dybczyński (1994), Breiter et al. (1996), Dybczyński & Prętko (1996, 1997).

### 3. Observable comets produced by the Galactic disk tide alone

In numerical simulations described in this paper we use the same two numerical models of the cloud, as described in Paper I. The first one, called DQT, is based on the classic paper (Duncan et al. 1987) on Oort cloud formation. The second one (called DLDW) is based on more recent simulations of the early stages of the planetary system, carried out by Luke Dones and his colleagues (Dones et al. 1998, 2000a,b). A detailed description and comparison of these two models can be found in Paper I, but key characteristics are worth mentioning here:

1. The DQT model is spherically symmetric, while the DLDW one is significantly flattened in its inner part (up to 10 000 AU) towards the invariant plane of the Solar System.
2. In the DQT model the inner part is much more populated than the outer part of the cloud. The situation is the opposite in the DLDW model. Its radial density profile has a maximum at 30 000 AU from the Sun, while for DQT this maximum occurs at 3000 AU.

As mentioned above, Galactic perturbations can change cometary orbits and make them observable without any additional perturbing forces. To observe the efficiency of such a process and to note any characteristics of the observed population obtained, we performed numerical simulations of the dynamical evolution of the cometary cloud under the galactic disk tide. Because the typical period of the long term changes is on the order of  $10^9$  years, it is necessary to follow the motion of each comet for at least  $10^{10}$  years to observe the full period of orbit evolution. Such a simulation can be substantially speeded up by using the appropriate “dynamical filter” (described below in Sect. 5), which allows us to concentrate on the “promising” cases based on the initial conditions. As a result, the motion of only about one tenth of the whole cloud population has to be integrated numerically.

Additionally, because we cannot account directly for planetary perturbations over such huge time intervals, it is convenient to use an additional parameter, measuring the “transparency” of the planetary system, first proposed in Dybczyński & Prętko (1997) and extensively discussed by Dybczyński (2004). This “planetary system transparency coefficient” ( $P$ ) describes the probability that a comet will be removed from

the cometary cloud by planetary perturbations during the single perihelion passage. The correct value of  $P$  is a complicated function of the cometary orbital elements, mainly the semi-major axis. Dybczyński (2004) estimated its value for different groups of comets using observed, cloned, and simulated comets. He obtained  $P \approx 0.25$  for comets from the inner part of the Oort cloud and  $P \approx 0.5$  for outer part comets.

In Fig. 1 one can inspect the flux of observable comets produced by the galactic disk tide. We used the DLDW model of the cloud in this case, but its flattened inner part did not manifest in any way. Because we included a planetary system transparency coefficient in the simulation the number of observable comets decreases slowly with time so that comets are slowly removed from the observable (i.e. perturbed by planets) part of the cloud. After the first 50 mln years the influx reaches its maximum value of approximately 80 comets per mln years, which when scaled to the cloud of  $10^{12}$  proto-comets, gives about 20 new comets with perihelia below  $OL = 5$  AU per year, close to the current estimates of the observed influx. This level of approximation is quite satisfactory here as the simulation is significantly simplified. We used here: constant disk matter density  $\rho$  over a long time interval, a completely thermalized cometary cloud without any imprints of recent perturbations, a simplified galactic perturbation model (disk tide only), and a highly simplified planetary perturbations model. The same simulation performed for the DQT model of the cloud resulted in the same but less populated distribution, and the influx obtained was less than one fourth of that for the DLDW model. Because the planetary system transparency can be applied after the main simulation, we checked the simulation output for different values of  $P$ . If we take the influx observed for  $P = 0$  (planetary system completely transparent) as 100%, for  $P = 0.5$  the influx is reduced to 25% and it goes down to 12% for  $P = 1$ , when each comet is removed after the first passage below 15 AU. A time interval of 500 mln years is used here only to ensure the complete independence of the initial cloud state, while we do not pretend to reproduce the real dynamical evolution of cometary orbits during such a long time. For this purpose (among others), a more sophisticated Galactic perturbation model should be used.

### 4. Mixing stellar and galactic perturbations

The stellar and galactic perturbations cannot be simply added. Instead, one has to develop a dynamical model for calculating the resulting effect, accounting for both perturbing agents in a simultaneous manner, as demonstrated by Matese & Lissauer (2002).

When analyzing the output of the single stellar passage under the simultaneous perturbations from the galactic disk tide, it is necessary to follow the motion of each comet numerically recording all its perihelion passages in the solar neighbourhood. The starting point for such a numerical integration is a result of the stellar impulse applied on each comet in the simulated cloud. As described in detail in Paper I, we calculate the complete effect of the stellar passage by means of the improved impulse approximation derived by Dybczyński (1994). After obtaining the new cometary orbit, we integrate

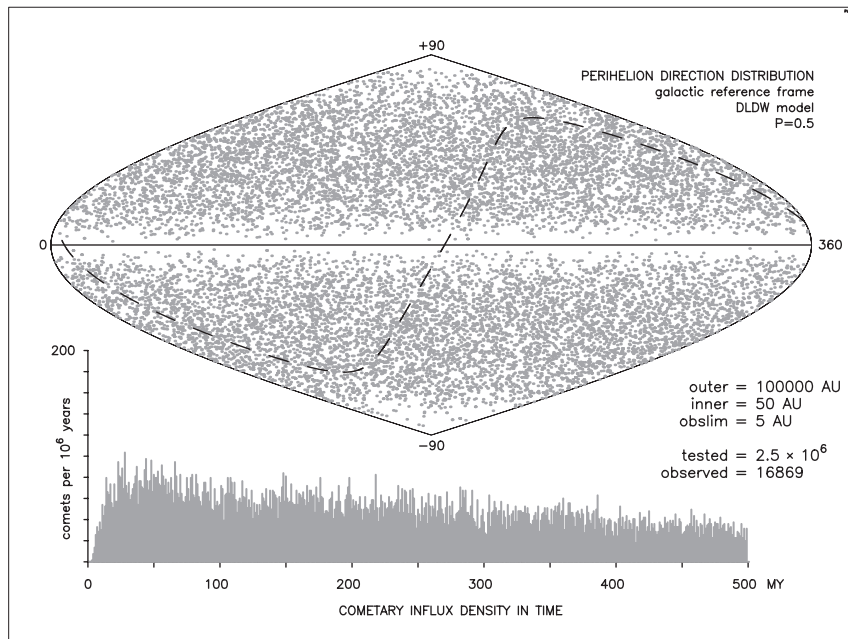


**Fig. 1.** The results of the numerical simulation of producing observable comets with galactic disk tide in the absence of any other perturbing forces. The upper part of this figure describes the distribution of the perihelion directions of observable comets on the celestial sphere in the galactic reference frame. The DLDW model of the cloud was used here. The dashed black line denotes the Solar System invariable plane orientation. One cannot observe any concentrations towards this plane – the flattened inner part of the DLDW model does not manifest in the observable population. In the lower part the obtained observable cometary influx versus time is presented.

its equations of motion numerically in rectangular coordinates in the form of Eqs. (1). For testing purposes we used several different numerical integrators. Due to the relatively simple right-hand sides of these equations, the fastest one was the high order Runge-Kutta-Dormand scheme (Dormand & Prince 1978) with automatic step-length adjustment. Our computer code for this method is based on the original *D2RKD7* routine developed by Fox (1984). As the control method we most often used the *RA15* routine (Everhart 1985).

The main difficulty which arises in this simultaneous treatment of the Galactic and stellar perturbations is the necessity for a large number of long numerical integrations, what makes such calculations time-consuming. With the aid of the so-called “*dynamical filtering*”, described in the next section, it is possible to speed the calculations up significantly but only for the single stellar passage. After the stellar perturbation calculation, we can “filter out” most of the comets from the cloud and numerically integrate only the remaining 10% or so. If we want to study several subsequent stellar passages, it would be necessary to integrate the motion of all of them numerically for most of the time, because the dynamical filter can be applied only after the last passage. Such a calculation would be extremely time-consuming, but we plan to perform some simulations of several stellar passages in the future. Meanwhile, we concentrate on modelling of results of the single passage and searching for any possible fingerprints of a perturbation that can be observed in the observable comet sample during the first several million years after the passage.

## 5. Dynamical filtering

Before we describe our Monte Carlo simulation scheme we present a very useful method for obtaining the minimum possible perihelion distance of a comet during its long-term dynamical evolution under the galactic disk tide. To this aim we use the analytical solution of averaged equations of a comet

motion derived in Breiter et al. (1996). Given the angular momentum vector  $\mathbf{C} = (c_x, c_y, c_z)^T = \mathbf{r} \times \dot{\mathbf{r}}$  and the Laplace vector  $\mathbf{A} = (a_x, a_y, a_z)^T = \dot{\mathbf{r}} \times \mathbf{C} - \mu \frac{\mathbf{r}}{r}$  of a comet ( $\mu$  defined by Eq. (2)), it is easy to calculate its eccentricity  $e = A/\mu$  and parameter  $p = C^2/\mu$ . With auxiliary variables:

$$\alpha = \frac{c_z^2(1 - e^2)}{C^2}, \quad (3)$$

$$\beta = (a_x^2 + a_y^2 - 4a_z^2)/\mu^2, \quad (4)$$

$$\kappa = (4 - 5\alpha + \beta)^2 + 20\alpha\beta, \quad (5)$$

one can calculate the maximum possible value of this comet eccentricity

$$e_{\max} = \frac{1}{8} \sqrt{4 - 5\alpha - \beta + \sqrt{\kappa}}, \quad (6)$$

and then its minimum possible heliocentric distance:

$$r_{\min} = \frac{p}{(1 - e^2)}(1 - e_{\max}). \quad (7)$$

Instead of using Eqs. (3) and (4), variables  $\alpha$  and  $\beta$  can also be obtained directly from cometary keplerian orbital elements:

$$\alpha = (1 - e^2) \cos^2 i, \quad (8)$$

$$\beta = 1 - \alpha - \sin^2 i(1 - e^2 + 5e^2 \sin^2 \omega). \quad (9)$$

We use Eq. (7) twice as the so-called dynamical filtering during our simulation, in a completely different manner: first to eliminate all comets that could have passed among planets in the past (filtering randomly generated initial conditions) and then, after applying the stellar impulse, to decide whether we should integrate the comet future motion or whether it is useless because *OL* cannot be reached. In the simulation presented in Fig. 1 we did not use the first filtering because in this case we wanted to observe the effect of the Galactic tide alone.

The same formulas as presented above may be used to filter out comets that go too far during their orbit evolution and thence are treated as “lost” from the cloud. An equivalent criterion may also be derived from the solution proposed by Matese & Whitman (1989), while the formulas proposed by Maciejewski & Prętko (1998) provide a rough estimation only but are thus less effective in this case.

## 6. Monte Carlo simulation scheme

As the main purpose of this paper is to demonstrate the results of a single stellar passage through or near the Oort cometary cloud under the simultaneous influence of galactic perturbations, we found it necessary to separate the sample of comets observable due to the effect in question from the background of observable comets produced by the galactic tide alone. We performed such a separation by means of the dynamical filtering described above. This filter allows us to reject all comets that can become observable without the stellar action. In this situation we have a steady state cloud model modified in such a manner that no comet can be observed under the galactic perturbation at any time. Then we apply the stellar impulse, which makes some comets observable without the need of any additional perturbations and, at the same time, stirs the whole cloud, transferring some other comets into the region of the phase space from which they might be observable later due to the disk tide action. This is admittedly a rather artificial model. It corresponds to the situation where stellar passages are well separated in time and do not overlap (which is not true in reality) and all observable comets are removed by planetary perturbations prior to the stellar passage. However, such a model allows detailed observations of population of observable comets induced by a single stellar passage combined with the subsequent Galactic disk tide perturbations. Thus the  $r_{\min}$  criterion (calculated from Eq. (7)) is used twice (in opposite ways and with different threshold values) in the simulation scheme presented below.

Our numerical simulation code uses several parameters defining the problem: inner ( $IB$ ) and outer ( $OB$ ) boundaries of the cometary cloud, “virgin boundary” ( $VB$ ) – the minimum heliocentric distance for which a comet may still be treated as not perturbed by the planets (i.e. it still belongs to the Oort cloud), “lost boundary” ( $LB$ ) – the maximum heliocentric distance behind which a comet is treated as lost from the cloud and the observability limit ( $OL$ ). In all simulations presented in this paper, we used:  $IB = 50$  AU,  $OB = 100\,000$  AU,  $VB = 15$  AU,  $LB = 150\,000$  AU, and  $OL = 5$  AU.

In our numerical simulation code used to obtain Figs. 5–7, we applied the following scheme:

1. Choose arbitrary parameters of the stellar passage, i.e. angular elements of the hyperbolic star orbit with respect to the Solar System barycenter (defined in the galactic frame), the mass of the star  $M_{\star}$ , its velocity at infinity  $V_{\infty}$ , and its perihelion distance  $q_{\star}$ , all kept constant in a single simulation.
2. Take random cometary elements from the adopted cloud model (DQT and DLDW models mentioned above were used interchangeably). Angular elements  $\omega$ ,  $\Omega$ , and  $M$  were always taken from the uniform distributions, as well as  $\cos i$  in DQT model.
3. If  $q < IB$  or  $Q > OB$  – *REJECT*.
4. First dynamical filtering: if  $r_{\min} < VB$  – *REJECT*. This comet should not appear in our simulation, because it has already visited the inner planetary region several times in the past. Such comets are most probably removed from the cloud by planetary perturbations (assuming  $P > 0$ ).
5. Calculate new comet orbit after accounting for the stellar perturbation, using the improved impulse approximation (Dybczyński 1994).
6. Second dynamical filtering: if  $r_{\min} > OL$  – *REJECT*. This comet cannot be made observable by galactic tide in any time, numerical integration of its motion is not necessary.
7. Follow the heliocentric motion of a comet under the influence of the tidal disk force by means of the exact numerical integration in rectangular coordinates (Eqs. (1)). Record cometary orbital elements at each moment of crossing the heliocentric sphere of radius of 15 AU. Stop the integration after 20 mln years.
8. Repeat steps from 2 to 7 until the statistically significant sample of observable comets is accumulated.

When using the DLDW model, due to its flattened inner part, the cometary orbital elements chosen in Step 2 are defined in the invariable plane frame and then transferred to the galactic frame for the rest of calculations.

In simulations performed to obtain results presented in Figs. 2–4, the filtering in Step 4 was omitted; instead some additional initial relaxation of the cometary cloud was added to avoid initial lack of observable comets, visible in Fig. 1 (first 50 mln years).

The effect of planetary perturbations described in Sect. 3 is completely ignored during simulation (except for the indirect account for the past perturbations, Step 4.) and applied only in post-processing (analyzing and plotting) of the data obtained. In the final data sets we record comet orbital elements at each perihelion passage below 15 AU. As a result, at the analysis stage we can apply different values of the “transparency coefficient”  $P$  and different observability limits (5, 3 or 1 AU) without repeating the time-consuming simulation calculations. The only disadvantage to this approach is producing huge output files that contain cometary elements at all perihelion passages below 15 AU.

## 7. General stellar effect on the cloud

The dynamical filtering described above (see also Breiter et al. 1996) may also be used as a tool for examining the overall effect of a stellar passage. Such an approach is very efficient because it is not necessary to integrate any orbits numerically and it gives an overestimation of the size of the observable part of the cloud of only few percent. When applied to DQT and DLDW cometary cloud models, before the stellar passage it gives very similar sizes of the potentially observable part of the cloud under the influence of the galactic disk tide, 6.2% and 6.0% respectively. This means that the probability that a

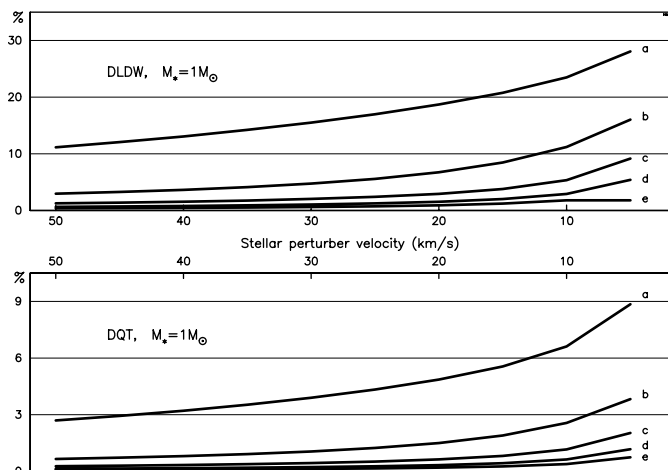


**Fig. 2.** The percentage of the observable part of the cometary cloud “refreshed” by the stellar passage as a function of the perturber velocity and proximity. *The upper panel* shows results for the DLDW model and the lower one for the DQT model of the cloud. In both cases, stellar mass equals that of the Sun. Curves a, b, c, d, and e describe results for  $q_* = 10, 30, 50, 70,$  and  $90$  thousand of AU, respectively. Note the different vertical scales of these two panels in this figure and the next one.

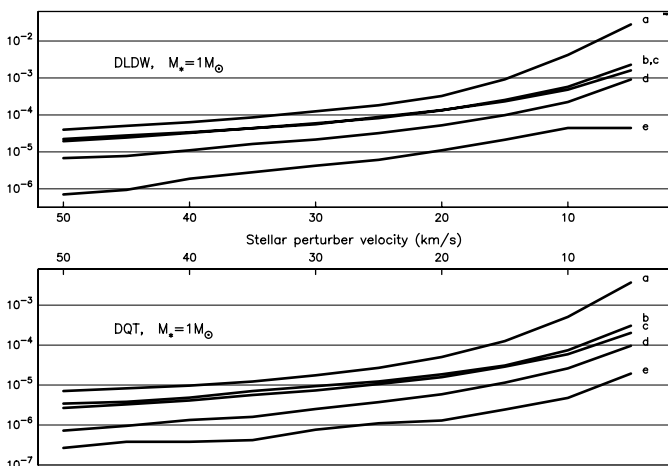


**Fig. 3.** The fraction of the whole cloud removed (i.e. transferred to the “lost” state, see text) after the stellar passage. *The upper panel* shows results for the DLDW model and the lower one for the DQT model of the cloud. Again curves a, b, c, d, and e describe the results for the Sun–star minimal distance  $d_* = 10, 30, 50, 70,$  and  $90$  thousand of AU, respectively.

comet will be observable (i.e. the perihelion distance will become lower than the assumed observability limit  $OL$ ) is on the order of 0.06 if we wait long enough, the period of the long term orbit variations due to the Galactic tide is on the order of  $10^8$ – $10^{10}$  years.

What is really surprising, after the stellar passage (of any tested mass, velocity, and geometry) the size of this observable part of the cloud remains the same. The only effect of the stellar perturbation is the replacing a small percent of this part with new comets taken from the initially unobservable part. One can observe this effect in Fig. 2 for both cloud models and different stellar velocities and proximity distances. As a result, the

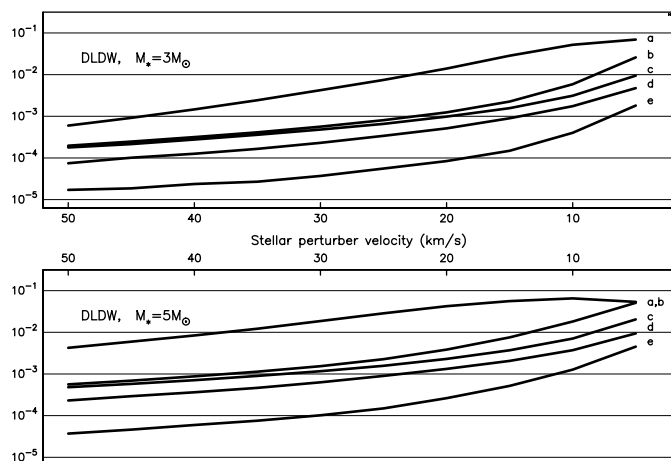


**Fig. 4.** Dependence of the removed fraction of the whole cloud on the mass and velocity of the stellar perturber. The upper panel shows results for the  $M_* = 3 M_\odot$  and the lower for  $M_* = 5 M_\odot$ . Both simulation series were performed for the DLDW model of the cloud. Again curves a, b, c, d, and e describe results for the Sun–star minimal distance  $q_* = 10, 30, 50, 70,$  and  $90$  thousand of AU, respectively.

probability of being observed does not change due to the stellar passage, the only effect being some asymmetries in apside line direction distributions and variations in the observable cometary influx with time. The remarkable difference between the two cloud model’s results comes from the fact that in the DLDW model most comets reside in the outer part of the cloud and are more sensitive to stellar perturbations.

The second result of the stellar perturbation is that a fraction of the whole cometary cloud is lost. Some cometary orbits become hyperbolic, while the aphelion distances of the others become larger than the outer limit of the cloud  $OL$ . This fraction of lost comets is different for the two models of the cloud used in this paper, and in both cases it depends on the stellar perturber mass and velocity, see Figs. 3 and 4. Note that even for very strong (and extremely rare) perturbations (large stellar mass with small velocity and deep penetrating passage), this lost fraction does not exceed 10%.

Again the difference between the results obtained for DQT and DLDW models comes from the different structures of these models, shown in detail in Paper I. The DQT model consists of a much more numerous inner part of the cloud, almost immune to stellar perturbations, so the percentage of lost comets is considerably smaller in the case of DQT.

## 8. Perihelion direction distribution of simulated observable comets and the time-dependence of their influx

In Paper I we presented three examples of the perihelion direction distribution of observable comets induced by stellar passages for  $q_* = 30\,000, 60\,000,$  and  $90\,000$  AU. The same three cases are presented in this paper for a simultaneous stellar and galactic perturbations model. The corresponding perihelion direction distributions, as well as the cometary influx time-dependence, are presented in Figs. 5–7. The format of these pictures is the same as in Paper I: the upper part presents

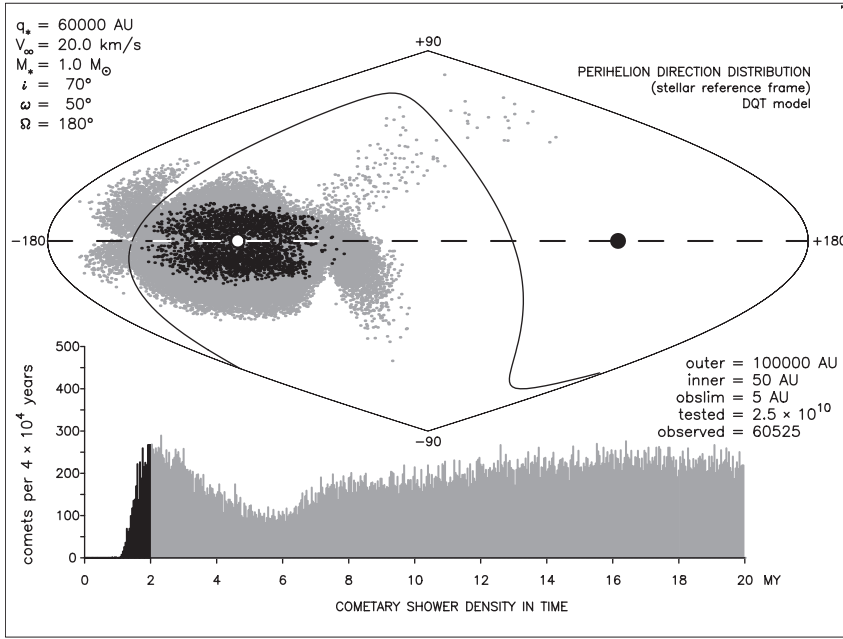


**Fig. 5.** Results of the numerical simulation of producing observable comets with stellar impulse and galactic disk tide acting simultaneously. The upper part of this figure describes the distribution of the perihelion directions of observable comets on the celestial sphere in the “stellar” reference frame. The parameters of the star and its passage are shown in the upper left corner. The dashed black line represents the projection of the star heliocentric orbit plane; star perihelion and anti-perihelion directions are marked with full and empty circles, respectively. The continuous black line denotes the position of the galactic disk plane. In the lower part, the obtained observable cometary influx versus time is presented. To be compared directly with Fig. 7 of Paper I.

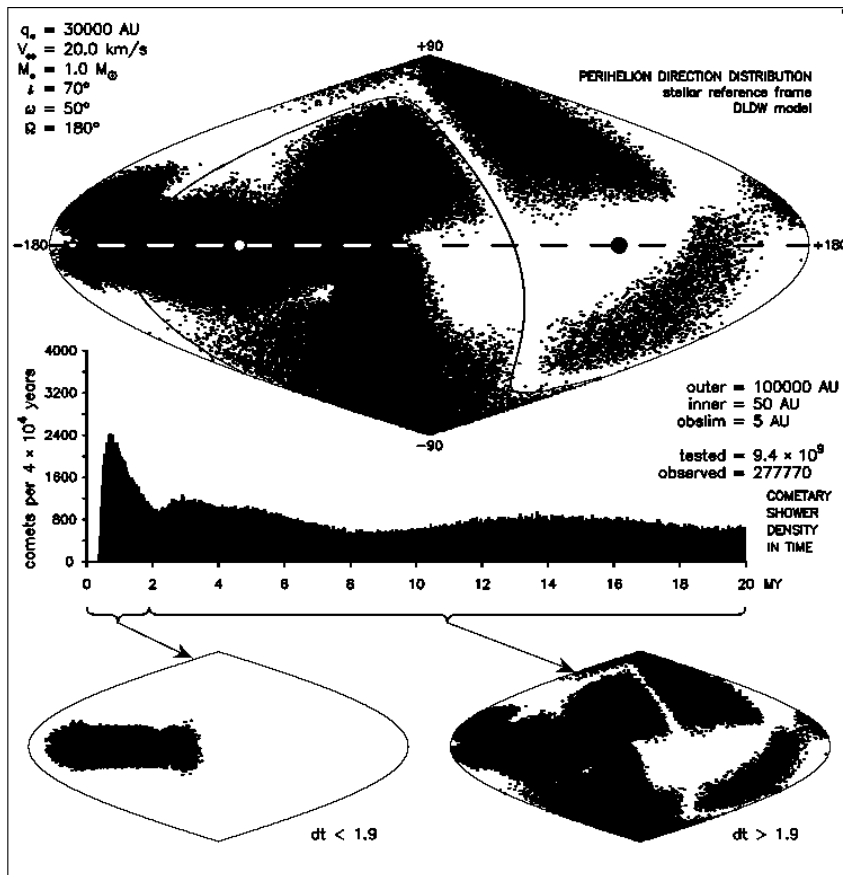


**Fig. 6.** Results of the numerical simulation of producing observable comets with stellar impulse and galactic disk tide acting simultaneously. In this example the output of the strong stellar perturbation with  $q_* = 30\,000$  AU is presented. Because of the high efficiency of such an event, we included two additional copies of the directional distribution of perihelion points for two separate time intervals at the bottom of this figure. High concentration of perihelion points in the first 2 mln years is thus clearly visible. Note the characteristic deficiency of perihelion points near the Galactic equator (solid curve in upper part plot). To be compared directly with Fig. 8 of Paper I.

the equal-area plot of the perihelion direction distribution on a celestial sphere, while the lower part consists of the histogram of the observable comet influx versus time. In Fig. 6 there is an additional part of the plot; the perihelion direction distribution is repeated at the bottom of the figure for two different time intervals. Because in each simulation we followed numerically the motion of a comet under the influence of the galactic disk

tide for 20 million years after the stellar passage and checked whether a comet becomes observable or not, we changed the scale of the horizontal axis of the flux histograms. To compensate for this (as well as for the simulated cloud population change for  $q_* = 60\,000$ ) in Figs. 5–7, we also changed the vertical scale so the lower part histograms can be directly compared with the corresponding plots in Figs. 7–9 of Paper I. The

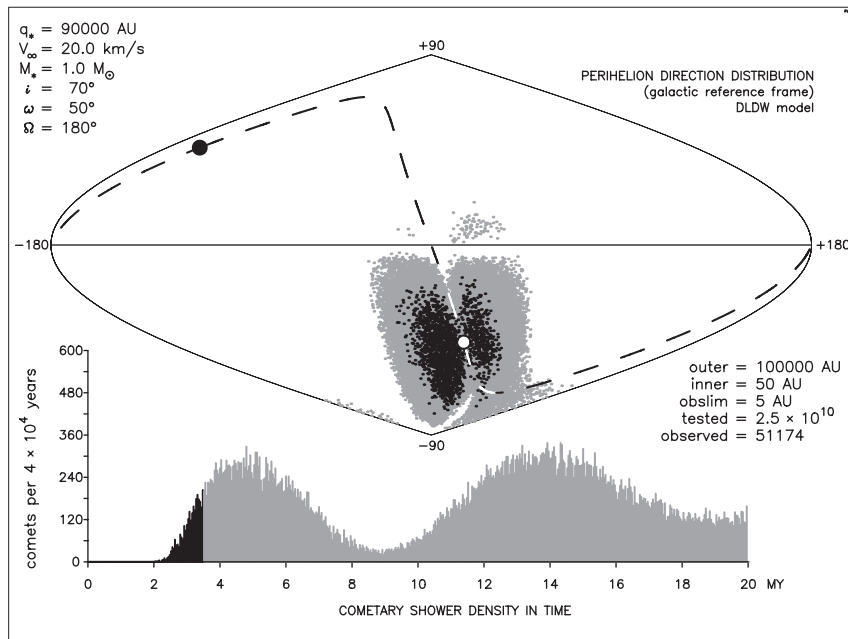


**Fig. 7.** The third example the simulation of producing observable comets with stellar impulse and galactic disk tide acting simultaneously, to be compared directly with Fig. 9 of Paper I. It is the case of rather weak (and the most probable) stellar action for  $q_* = 90\,000$  AU. The upper plot is presented in the Galactic frame; the straight solid line represents the galactic equator, while the dashed curve represents the heliocentric star orbit plane. In the flux histogram, two consecutive maxima of the same value are clearly shown. They are separated by approx. 9 mln years. A very deep minimum of observable cometary flux occurs 9 mln years after the stellar passage.

orientations of the upper part plots were also kept the same. The heliocentric orbit parameters of the stellar perturber with respect to the Galactic frame are shown in the left upper corner of each of these figures.

The highly concentrated distributions obtained in all cases in Paper I are spread more in the present model due to the galactic perturbations. But the subsample of comets, observable shortly after the stellar passage, remains concentrated near the anti-perihelion of the star heliocentric orbit in the same manner as in Paper I. It means that if we know the geometry of the stellar passage, we can predict the region of the celestial sphere occupied by the perihelion directions of the observable comets during the first maximum of the flux induced by the stellar perturbation.

In all three examples the flux of observable comets decreases after the first peak (located almost exactly at the same time as in Paper I), then rises again due to the galactic tide perturbations and continues long after the stellar passage. The maximum flux in the first peak appears to be a little smaller in the present model than obtained for the separate stellar perturbation in Paper I. It means that the perihelion distances of some comets placed in the observable part of the cloud, due to the stellar passage, evolve first towards higher values than to the observability limit  $OL$  before the first visit among planets and these comets will be observable much later.

It should be noted here that the results presented in Figs. 5–7 are somewhat filtered: in our simulation scheme we removed any potentially observable comets (due to the Galactic tide) from the cometary cloud before the stellar passage occurs. This was done to separate any fingerprints of the stellar perturbation from the background of the comets observable due to the galactic action. As mentioned in the previous section, the overall number of observable comets does not change after the stellar passage, so any stellar fingerprints are limited to the presented asymmetries and variations of the cometary influx with time.

In Paper I we presented distributions of the semi-major axes of the observable comets for three presented examples of stellar passages. They remain almost unchanged in the present model of mixed stellar and galactic perturbation; therefore, we do not present them here and the interested reader is directed to Paper I.

## 9. Conclusions

We presented results of simulations of stellar passages through or near the Oort cometary cloud under the simultaneous action of the galactic disk tide. The result of the stellar perturbation for different geometries, masses, and velocities of the perturber and for two different cloud models, is described.

The main conclusions are:

1. The stellar passage does not change the size of the observable (due to the Galactic tide) part of the cloud. As a result, the long-term average flux of the observable comets remains the same, even for close passages and strong stellar perturbations.
2. The only fingerprint of the stellar action is the asymmetry of the distribution of the perihelion directions of comets observable after the passage and short term variations of the influx of observable comets.
3. For comets observable shortly after the stellar passage, the distribution of the perihelion directions remains highly concentrated around the anti-perihelion point of the stellar heliocentric orbit even under the Galactic disk tide action, which directly confirms the result obtained in Paper I.
4. The flux of observable comets after the stellar passage starts with the same maximum as in the absence of the Galactic tide. Then, after a significant decrease, it rises again in contrast to the pure stellar effect presented in Paper I.
5. The fraction of the observable part of the cloud “refreshed” by the stellar passage is typically a few percent and, even for very strong stellar perturbation, does not exceed 10%.

6. The DLDW model of the cloud is much more sensitive to stellar perturbations because of a more numerous outer part. Its flattened inner part did not manifest in the results.

The results presented in this paper are important for investigating of the possible fingerprints of the recent stellar passage near or through the Oort cometary cloud. On the basis of these results, it is possible to define the conditions to be fulfilled by a star when searching for a recent perturber in stellar catalogs. They might also be of great help when filtering the observed sample of the long-period comets to find those recently perturbed and made observable by a passing star. Work on it is in progress.

*Acknowledgements.* The research described in this paper was supported by KBN grant No. 2P03D01324. This manuscript was prepared with L<sup>A</sup>T<sub>E</sub>X, the open source front-end to the T<sub>E</sub>Xsystem.

## References

- Brasser, R. 2001, MNRAS, 324, 1109  
 Breiter, S., Dybczyński, P. A., & Elipe, A. 1996, A&A, 315, 618  
 Byl, J. 1983, The Moon and the Planets, 29, 121  
 Byl, J. 1986, Earth, Moon and Planets, 36, 263  
 Dones, L., Duncan, M. J., Levison, H. F., & Weissman, P. R. 1998, in AAS/Division of Planetary Sciences Meeting, 30, 5107  
 Dones, L., Levison, H., Duncan, M., & Weissman, P. 2000a, Formation of the Oort Cloud, pers. comm.  
 Dones, L., Levison, H., Duncan, M., & Weissman, P. 2000b, in AAS/Division of Planetary Sciences Meeting, 32, 3602  
 Dormand, J. R., & Prince, P. J. 1978, Celest. Mech., 18, 223  
 Duncan, M., Quinn, T., & Tremaine, S. 1987, AJ, 94, 1330  
 Dybczyński, P. A. 1994, Celest. Mech. Dyn. Astron., 58, 139  
 Dybczyński, P. A. 2002a, Earth Moon and Planets, 90, 483  
 Dybczyński, P. A. 2002b, A&A, 383, 1049  
 Dybczyński, P. A. 2002c, A&A, 396, 283  
 Dybczyński, P. A. 2004, A&A, 428, 247  
 Dybczyński, P. A., & Prętko, H. 1996, Earth Moon and Planets, 72, 13  
 Dybczyński, P. A., & Prętko, H. 1997, in Dynamics and Astrometry of Natural and Artificial Celestial Bodies, ed. I. M. Wytrzyszczak, J. H. Lieske, & R. A. Feldman (Kluwer Academic Publishers), IAU Colloq., 165, 149  
 Everhart, E. 1985, in Dynamics of Comets: Their Origin and Evolution, ed. A. Carusi, & G. B. Valsecchi (D. Reidel Publishing Company), IAU Colloq., 83, 185  
 Fox, K. 1984, Celest. Mech., 33, 127  
 Harrington, R. S. 1985, Icarus, 61, 60  
 Heisler, J., & Tremaine, S. D. 1986, Icarus, 65, 13  
 Holmberg, J., & Flynn, C. 2000, MNRAS, 313, 209  
 Levison, H. F., Dones, L., & Duncan, M. J. 2001, AJ, 121, 2253  
 Maciejewski, A. J., & Prętko, H. 1998, A&A, 336, 1065  
 Matese, J., & Whitmire, D. 1996, APJ, 472, L41  
 Matese, J. J., & Lissauer, J. J. 2002, Icarus, 157, 228  
 Matese, J. J., & Whitman, P. G. 1989, Icarus, 82, 389  
 Oort, J. H. 1950, Bull. Astron. Inst. Nether., 11, 91  
 Prętko, H. 1998, in IV International Workshop on Positional Astronomy and Celestial Mechanics, ed. A. Lopez Garcia et al. Astronomical Observatory, University of Valencia, Spain, 249  
 Prętko, H., & Dybczyński, P. A. 1994, in Dynamics and Astrometry of Natural and Artificial Celestial Bodies, ed. K. Kurzyńska, F. Barlier, P. K. Seidelmann, & I. Wytrzyszczak, Astronomical Obs. of the A.Mickiewicz Univ., Poznań, Poland: Astronomical Obs. of the A.Mickiewicz Univ., 299